Electronic states and photoluminescence of TiO_2 nanotubes with adsorbed surface oxygen

L. Z. Liu,[1] W. Xu,[1] X. L. Wu,[1,a)] Y. Y. Zhang,[1] T. H. Chen,[2] and Paul K. Chu[3,a)]
[1]*National Laboratory of Solid State Microstructures and Department of Physics, Nanjing University, Nanjing 210093, People's Republic of China*
[2]*College of Physics Science and Technology, Yangzhou University, Yangzhou 225002, People's Republic of China*
[3]*Department of Physics and Materials Science, City University of Hong Kong, Tat Chee Avenue, Kowloon, Hong Kong, China*

(Received 14 January 2012; accepted 1 March 2012; published online 20 March 2012)

The electronic states associated with enhanced photocatalytic activity of anodic anatase TiO_2 nanotubes (NTs) annealed in N_2 and O_2 are investigated by photoluminescence (PL). The NTs annealed in N_2 show a green peak related to oxygen vacancies and its position blueshifts with deceasing temperature, whereas those annealed in O_2 show a double peak at 475–600 nm and the energy separation increases with decreasing temperature. Spectral analysis and density function theory calculation disclose that the double peak results from residual oxygen vacancies and oxygen atoms on the NT wall and the increased energy separation arises from the larger difference between the inner and outer NT stress at low temperature. © *2012 American Institute of Physics*. [http://dx.doi.org/10.1063/1.3695167]

Ti oxide nanostructures have attracted much attention because of their interesting applications such as gas sensing, solar-to-chemical conversion (water splitting), and environment cleaning (photodecomposition of harmful materials or dirt).[1–5] Their properties depend very much on the surface structure and reactant adsorption. Nanostructures such as nanotubes (NTs), nanocrystals (NCs), nanodisks, and nanowires have been fabricated and their optical and electronic characteristics and potential applications have been explored.[6–9] The NT structures with a large surface to volume ratio tend to yield excellent performance. TiO_2 has three common phases, namely, anatase, rutile, and brookite. Anatase and rutile are more relevant to many applications and between the two, anatase TiO_2 has attracted more interest especially in surface chemistry due to its higher catalytic activity.[10]

In many energy and environment related applications, improved efficiency and stability are required and a better understanding of the related mechanism is thus crucial. It has been shown that oxygen adsorption onto the nanostructure surface can effectively modify the reaction captivity[11,12] and, therefore, it is important to clarify the oxygen mechanism. However, the complexity of the nanostructure and lack of systematic theoretical assessment make it challenging. Photoluminescence (PL) can reflect the interaction between the electronic states of a nanostructure with vacancy structure and adsorptive reactants and there has been extensive research to identify its origin.[5–7] The sensing properties of TiO_2 are generally based on sensitive transduction of the gas/surface interaction (adsorption or catalytic oxidation) into electrical conductivity.[13,14] If the PL origin of the nanostructure with adsorptive oxygen can be identified experimentally and theoretically, this mechanism can be applied to oxygen sensing by simply analyzing the PL spectral change. In this respect, the low-temperature PL spectral changes in anatase TiO_2 NTs with a vacancy structure and adsorbed oxygen should be clarified. The objective of this work is to identify and explain the PL properties of the TiO_2 NTs formed by anodic oxidation with both vacancy structure and oxygen adsorption to develop potential catalytic and sensing applications.

The TiO_2 NTs were formed by anodic oxidation of a Ti foil at 30 V and 10 °C in an ethylene glycol solution containing NH_4F (0.5 wt. %) for 5 h.[15] The sample was annealed in O_2 or N_2 at $T_a = 400$ °C for 30 min. The samples were characterized by scanning electron microscopy (SEM), high-resolution transmission electron microscopy (HR-TEM) (JEOL-2100), electron paramagnetic resonance (EPS) spectroscopy, UV-visible diffuse reflection spectroscopy (DRS), x-ray diffraction (XRD), PL excitation spectroscopy, and x-ray photoelectron spectroscopy (XPS). All the measurements were conducted at room temperature.

The SEM image acquired from the NT samples annealed at 400 °C in O_2 for 30 min is shown in Fig. 1(a), and the orderly self-organized NT array can be clearly observed. The average NT outer diameter (marked by blue dashed lines) is about 83 nm and the NT wall thickness (marked by black dashed lines) is approximately 8.5 nm. To clearly display this NT morphology, lateral SEM image of the NT array is shown in Fig. 1(b) and the length of the NTs is about several micrometers. Obviously, the huge internal space of the NTs can be effectively used for oxygen adsorption and sensing.

To further investigate the microstructures of the NTs annealed at 400 °C in O_2, more spectroscopic results are displayed in Fig. 2. The XRD pattern of the TiO_2 NTs on the Ti foil is given in Fig. 2(a) and compared to the JCPDS card NO. 21-1272.[15] An important difference is that the strongest diffraction peak of the TiO_2 NTs arises from (004) instead of (101) which is common in anatase TiO_2. It can be understood

a)Authors to whom correspondence should be addressed. Electronic addresses: hkxlwu@nju.edu.cn and paul.chu@cityu.edu.hk.

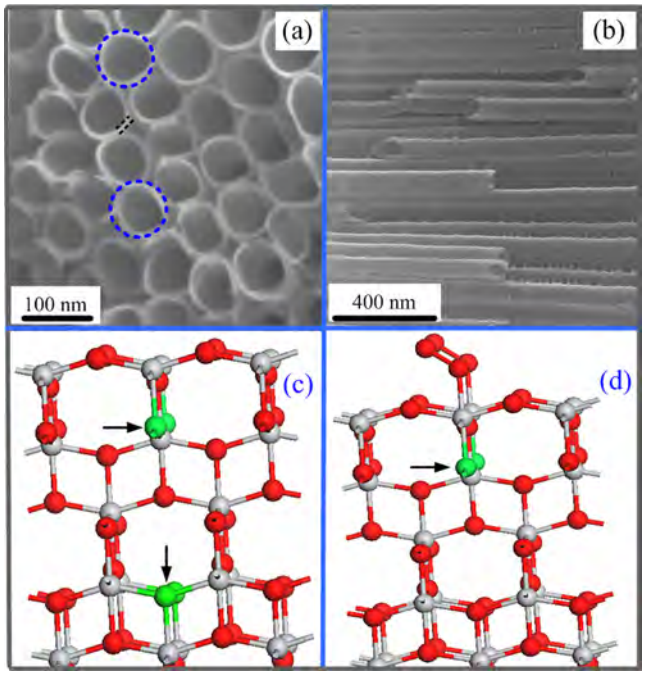

FIG. 1. (Color online) (a) and (b) SEM images (top and lateral views) of the anodic TiO_2 NTs annealed in O_2 at 400 °C. (c) and (d) One supercell structure of samples used in the DFT calculation for anatase TiO_2 films with (001) surface and with resident OVs (c) and oxygen adsorptions (d). The gray and red (black) balls represent Ti and O atoms and the green (by arrow) balls stand for oxygen atomic vacancies, respectively.

to be the dominant exposed (001) facet on the NT surface. The UV-visible DRS result is shown in the inset of Fig. 2(b).[15] By plotting the Kubelka-Munk function versus wavelength,[16] the bandgap of the anatase TiO_2 NT is derived to be about 3.38 eV [Fig. 2(b)], which is slightly larger than that of bulk TiO_2 (3.2 eV). In the anatase TiO_2 nanoparticle system, it has been reported that the excition Bohr radius R is about 0.8 nm and no shift in the bandgap energy has been observed for nanoparticles with a size of $2R \geq 1.5$ nm.[17] Therefore, this enlarged bandgap (3.38 eV) cannot simply be ascribed to quantum confinement in the TiO_2 NT, but rather it may originate from the NT adsorptive characteristics. The EPR spectrum in Fig. 2(d) indicates that electrons of the adsorbed oxygen atoms can be trapped by Ti^{4+} atoms on the NT wall to form the Ti^{3+} valence state. This changes the effective electron and hole masses and consequently causes a slight bandgap expansion of the NTs.[18–20] The Ti 2p XPS spectrum in Fig. 2(c) reveals that the binding energies of Ti $2p_{3/2}$ and Ti $2p_{1/2}$ are 459.2 and 465.1 eV, respectively. Compared to the binding energy of Ti^{4+} in pure anatase TiO_2 (458.6 eV), there is a shift of 0.6 eV, suggesting that some Ti^{3+} or Ti^{2+} still exist in the sample[21,22] and that OVs have not been removed completely despite annealing at 400 °C in O_2. To further investigate oxygen adsorption on the NT surface, the EPR signal is shown in Fig. 2(d). The Lande g value is obtained to be 2.0056 and larger than that of the sample with only OVs ($g = 2.003$).[22,23] Because the anion radicals O_2^- and/or O^- can be formed due to capture of thermally generated electrons and holes by adsorbed oxygen ($O_2 + e^- \rightarrow O_2^-$) during annealing, the concentration of O_2^- increases with adsorptive oxygen on the anatase TiO_2 surface. This makes the g factor larger.[23] The above analysis shows that the synthesized NTs have the anatase phase with a certain OV amount and meanwhile the NT walls are covered by adsorbed oxygen atoms.

Figure 3(a) shows the temperature-dependent PL spectra acquired from the anatase TiO_2 NTs annealed at 400 °C in N_2 excited by the 320 nm line of a xenon lamp. All the spectra show a visible green band at ~515 nm (2.41 eV) which has been assigned to OVs that are essential defects in metal oxides.[24,25] Its intensity increases gradually as the measurement temperature decreases due to weaker

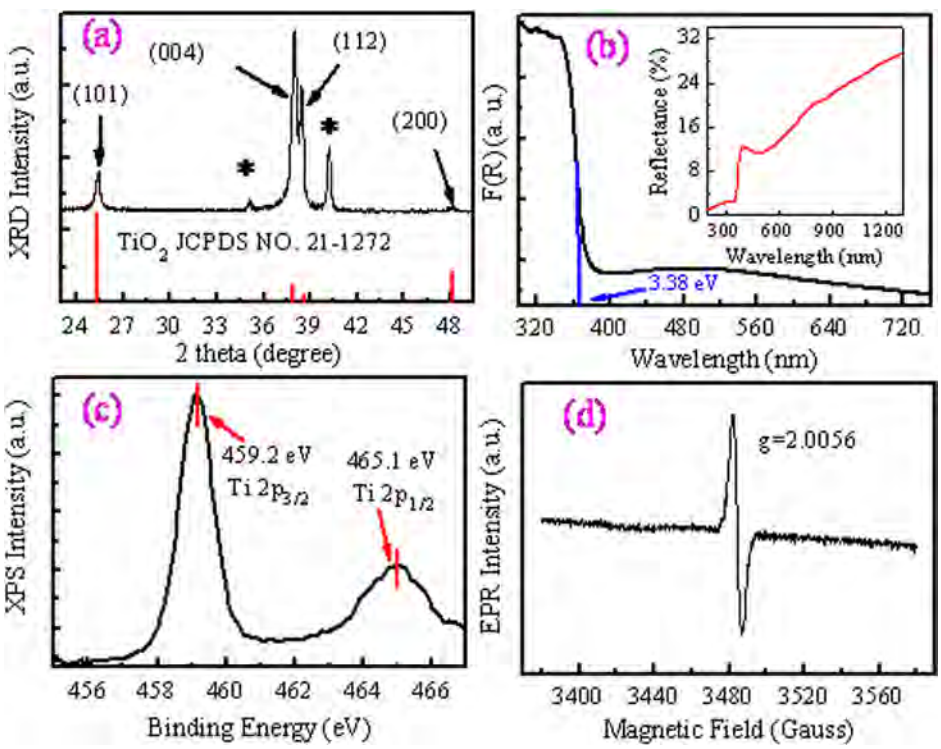

FIG. 2. (Color online) (a) XRD pattern of the TiO_2 NTs annealed in O_2 at 400 °C. The Ti foil substrate peaks are marked with (✱). (b) Calculated Kubelka-Munk function F(R) versus wavelength and the inset shows the corresponding UV-visible DRS. (c) and (d) Ti 2p XPS and room-temperature EPR spectra of the annealed NTs.

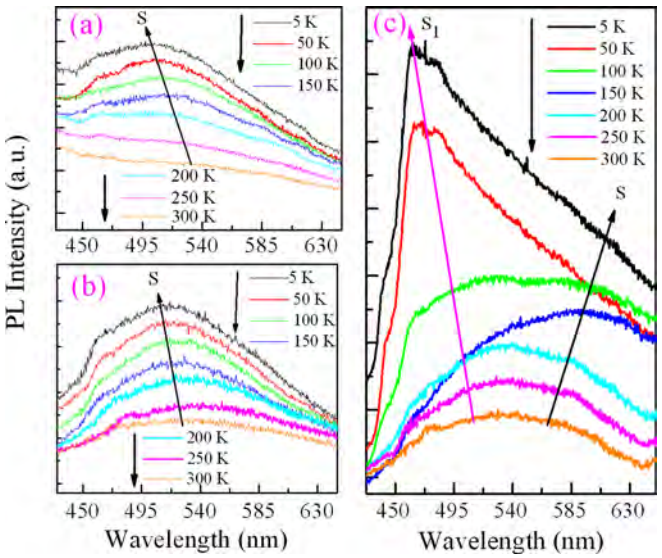

FIG. 3. (Color online) Temperature-dependent PL spectra acquired from the TiO_2 NT samples with (a) ~83 and (b) 105 nm diameters annealed in N_2 at $T_a = 400\,^{\circ}C$, and (c) ~83 nm diameter annealed in O_2 at $T_a = 400\,^{\circ}C$.

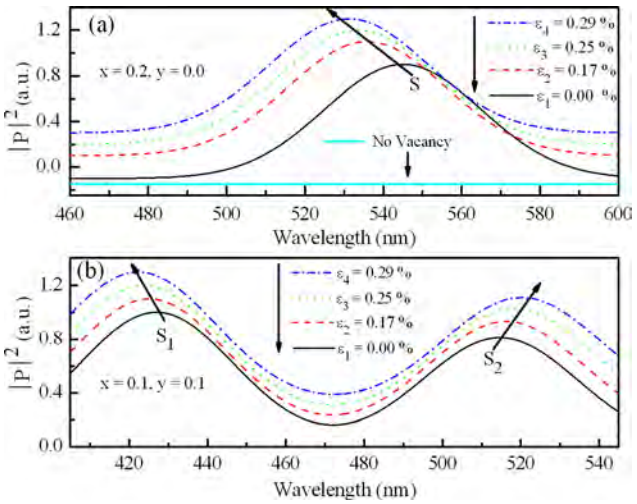

FIG. 4. (Color online) Calculated average squared optical matrix element as a function of energy for anatase TiO_2 films with (001) surface and with different OVs and oxygen adsorption under different applied stresses.

nonradiative recombination. Meanwhile, the peak position is up-shifted slightly and it can be ascribed to the NT curvature change induced by the internal stress due to the cool shrinkage effect. To clarify the mechanism, PL spectra are acquired from similar NT samples with larger outer diameters (~105 nm) and shown in Fig. 3(b). The smaller up-shift is attributed to the decreased curvature change in larger samples and consistent with our assessment. Figure 3(c) displays the corresponding PL results obtained from the sample annealed at 400 °C in O_2. Different PL features composed of a double-peak structure (S_1 and S) are observed as the measurement temperature decreases and the energy separation between two subpeaks increases. The linewidth and shape of the S subpeak are similar to those in Figs. 3(a) and 3(b) albeit the redshift. The S_1 subpeak has a small linewidth and blueshifts. Since residual OVs still exist after annealing in O_2 and oxygen adsorbs onto the NT wall [Fig. 2(c)], both the adsorbed oxygen atoms and intrinsic OVs may be responsible for the double-peak PL. The difference in the applied stress caused by oxygen adsorption on the inner and outer NT surfaces increases as the measurement temperature decreases and it causes increased splitting and shifting of the PL peak.

To understand the origin of the double-peak PL, we perform a density functional theory (DFT) study on the anatase TiO_2 film to investigate the effects of the inner OVs and surface oxygen adsorption as shown in Figs. 1(c) and 1(d) under different applied stress to simulate different curvature situation of NTs using the CASTEP package.[26] Here, all the films are carved along the (001) planes. The norm-conserving pseudopotential is used for the electron-ion interactions and the Perdew-Burke-Ernzerhof form of generalized gradient approximation is employed to describe the exchange-correlation functional.[27,28] A cutoff energy of 340 eV and regular Monkhorst-Pack grid $4 \times 2 \times 1$ k points are adopted to ensure energy convergence to within 1-2 meV/atom. Considering the inner OVs and adsorbed oxygen atoms on the surface, the structure becomes more complicated and its density of states is also modified correspondingly. The specific contribution of the complex surface states to electron-hole recombination can be investigated by computing the optical transition matrix element associated with surface states, which is defined by[29] $|P|^2(E) = \sum_{\vec{k},v,c} |\langle \psi^c_{\vec{k}}(\vec{r})|\vec{u}\cdot\vec{r}|\psi^v_{\vec{k}}(\vec{r}^{\rightarrow})\rangle|^2 \delta(E^c_{\vec{k}} - E^v_{\vec{k}} - E)$, in which E is the transition energy, $k^{\rightarrow}$ is the Bloch wave vector of the superlattice, $E^{c(v)}_{\vec{k}}$ and $|\psi^{c(v)}_{\vec{k}}(\vec{r})\rangle$ are the eigen-energy and wave function of the state in the conduction, respectively, $\vec{r}$ is the position vector, and $\vec{u}$ is the unit vector along the unpolarization of the light. As the measurement temperature decreases, the applied stress in the calculated models increases and it can be defined as $\varepsilon = (a_0 - a)/a_0$, and a and a_0 are the stressed and unstressed lattice constants.

Based on the model shown in Fig. 1(c) (only including OVs), the calculated averaged $|P|^2$ values are shown in Fig. 4(a). As the OV density increases from x = 0.0 to x = 0.2, an obvious peak (S) begins to appear at ~545 nm and then up-shifts to 530 nm with increasing stress from $\varepsilon_1 = 0.00\%$ to $\varepsilon_4 = 0.29\%$, which is consistent with the experimental measurements shown in Figs. 3(a) and 3(b). After annealing in O_2, partial OVs are removed and superfluous oxygen atoms adsorb on the surface near the OV positions to construct Ti-O bonds forming a more stable stoichiometric NT surface, as shown in Fig. 1(d). In this case of OV density x = 0.1 and adsorbed oxygen atom density y = 0.1, the calculated $|P|^2$ values shown in Fig. 4(b) reveal that introduction of surface states originating from adsorbed oxygen atoms separates the PL spectrum into two (S_1 and S). The energy separation between the two peaks increases with decreasing measurement temperature as a result of the larger difference between the inner and outer NT stresses, as shown in Fig. 3(c). The calculation suggests that surface oxygen adsorption changes the electronic structure and this may be responsible for the enhanced photocatalytic activity observed from annealed TiO_2 NT samples.[15] The difference between the experimental and theoretical PL wavelengths can be ascribed to the sample complexity.

In conclusion, anatase TiO_2 NTs with OVs are synthesized by anodic oxidation and then annealed in N_2 or O_2. The

low-temperature PL spectra reveal a single peak from the NTs annealed in N_2 and a double peak for those annealed in O_2. The energy separation between the two latter subpeaks increases as the measurement temperature decreases. Spectral analyses and theoretical calculation suggest that the double peak PL originates from both the residual OVs and adsorbed oxygen atoms on the NT wall and the increased energy separation is due to increased difference between inner and outer NT stresses during lower temperature measurement.

This work was jointly supported by grants (Nos. 2011CB922102, 11004170, and 60976063) from the National Natural Science Foundation and Basic Research Programs of China and Postdoctoral Science Foundations of China and Jiangsu Province (Nos. 2011M500889 and 1102001B). Partial support was also from PAPD and Hong Kong Research Grants Council (RGC) General Research Fund (GRF) No. CityU 112510.

[1]M. Sumita, C. P. Hu, and Y. Tateyama, J. Phys. Chem. C **114**, 18529 (2010).
[2]H. Katto, K. Asakura, and A. Kudo, J. Am. Chem. Soc. **125**, 3082 (2003).
[3]A. Fujishima, T. N. Rao, and D. A. Tryk, J. Photochem. Photobiol. C **1**, 1 (2000).
[4]W. Zeng, T. Liu, Z. C. Wang, S. S. Tsukimoto, M. Saito, and Y. Ikuhara, Mater. Trans, **51**, 171 (2010).
[5]A. L. Linsebigler, G. Q. Lu, and J. T. Yates, Chem. Rev. **95**, 735 (1995).
[6]K. S. Jeon, S. D. Oh, Y. D. Sun, H. Y. Yoshikawa, H. Masuhara, and M. Yoon, Phys. Chem. Chem. Phys. **11**, 534 (2009).
[7]D. V. Bavykin, S. N. Gordeev, A. V. Moskalenko, A. A. Lapkin, and F. C. Walsh, J. Phys. Chem. B **109**, 8565 (2005).
[8]J. M. Wu, H. C. Shih, and W. T. Wu, Nanotechnology **17**, 105 (2006).
[9]N. D. Abazović, M. I. Čomor, M. D. Dramićanin, D. J. Jovanović, S. P. Ahrenkiel, and J. M. Nedeljković, J. Phys. Chem. B **110**, 25366 (2006).
[10]E. Comini, M. Ferroni, V. Guidi, G. Faglia, G. Martinelli, and G. Sberveglier, Sens. Actuators, B **84**, 26 (2002).
[11]S. Ikeda, N. Sugiyama, B. Pal, G. Marcic, L. Palmisano, H. Noguchi, K. Uosaki, B. Ohtani, Phys. Chem. Chem. Phys. **3**, 267 (2001).
[12]R. Nakamura and Y. Nakato, J. Am. Chem. Soc. **126**, 1290 (2004).
[13]A. Kolmakov, Y. X. Zhang, G. S. Cheng, and M. Moskivits, Adv. Mater. **15**, 997 (2003).
[14]A. Ponzoni, E. Comini, G. Sberveglieri, J. Zhou, S. Z. Deng, N. S. Xu, Y. Ding, and Z. L. Wang, Appl. Phys, Lett. **88**, 203101 (2006).
[15]Y. Y. Zhang, X. L. Wu, L. Z. Liu, T. H. Li, and P. K. Chu, Appl. Phys. A **105**, 703 (2011).
[16]G. S. Pang, S. G. Chen, Y. Koltypin, A. Zaban, S. H. Feng, and A. Gedanken, Nano Lett. **1**, 723 (2001).
[17]S. Monticone, R. Tufeu, A. V. Kanaev, E. Scolan, and C. Sanchez, Appl. Surf. Sci. **162**, 565 (2000).
[18]L. Kavan, T. Stoto, M. Grätzel, D. Fitzmaurice, and V. Shklover, J. Phys. Chem. **97**, 9493 (1993).
[19]U. Hörmann, U. Kaiser, M. Albrecht, J. Geserick, and N. Hüsing, J. Phys.: Conf. Ser. **209**, 012039 (2010).
[20]C. Kormann, D. W. Bahnemann, and M. R. Hoffmann, J. Phys. Chem. **92**, 5196 (1988).
[21]X. W. Wang, G. Liu, L. Z. Wang, J. Pan, G. Q. Lu, and H. M. Cheng, J. Mater. Chem. **21**, 869 (2011).
[22]Y. Z. Li, D. S. Hwang, N. H. Lee, and S. J. Kim, Chem. Phys. Lett. **404**, 25 (2005).
[23]E. Konstantinova, J. Weidmann, and T. Dittrich, J. Porous Mater. **7**, 389 (2000).
[24]W. F. Zhang, M. S. Zhang, Z. Yin, and W. Chen, Appl. Phys. B **70**, 261 (2000).
[25]Y. X. Jin, G. H. Li, Y. Zhang, Y. X. Zhang, and L. D. Zhang, J. Phys.: Condens. Matter. **13**, L913 (2001).
[26]M. Vanderbilt, Phys. Rev. B **41**, 7892 (1990).
[27]D. R. Hamann, M. Schluter, and C. Chiang, Phys. Rev. Lett. **43**, 1494 (1979).
[28]J. P. Perdew, K. Burke, and M. Ernzerhof, Phys. Rev. Lett. **77**, 3865 (1996).
[29]H. T. Chen, S. J. Xiong, X. L. Wu, J. Zhu, J. C. Shen, and P. K. Chu, Nano Lett. **9**, 1926 (2009).